MATERIALS CHEMISTRY FRONTIERS

RESEARCH ARTICLE

View Article Online
View Journal | View Issue

Cite this: *Mater. Chem. Front.*, 2025, **9**, 3478

Simultaneous fluorescence-phosphorescence dual-emission based on phenoxathiin and polycyclic aromatic hydrocarbons towards temperature sensing

Yuling Huang,†[a] Huiwen Zeng,†[a] Yu Lang,[a] Cong Liu,[a] Zixuan Ran,[a] Fayong Li,[c] Jiadong Zhou,*[a] Bingjia Xu*[b] and Guang Shi*[a]

Received 19th August 2025,
Accepted 20th October 2025

DOI: 10.1039/d5qm00618j

rsc.li/frontiers-materials

Dual-mode fluorescence-phosphorescence emission materials have attracted significant attention due to their wide range of potential applications. However, it remains challenging to obtain organic dual-mode fluorescence-phosphorescence materials that are both highly efficient and long-lived. To investigate the impact of molecular structures on fluorescent-phosphorescent temperature probes, phenanthrene (Phen) and teriphenylene (TP), two polycyclic aromatic hydrocarbons, were introduced into the phenoxathiin (POX) unit, which exhibits a folding-induced enhanced spin–orbit coupling effect. The POX derivatives (POXPhen and POXTP) were doped as guest emissive molecules into melamine-formaldehyde polymer films, showing both highly efficient fluorescence and phosphorescence with phosphorescence quantum yields and lifetimes exceeding 20% and 1 second, respectively. Theoretical and experimental results demonstrate that different steric hindrance effects and van der Waals forces exerted by the Phen and TP groups on the POX unit lead to perturbed conformations involving the torsion angles between Phen/TP groups and POX fragments. These perturbed conformations impact the intersystem crossing process as well as fluorescence and phosphorescence processes. Notably, the molecular conformational distribution exhibits temperature reliability, and the temperature-dependent emission of POXPhen and POXTP demonstrates a good linear relationship between the phosphorescence to fluorescence intensity ratio and temperature, ranging from 9.25 °C to 110.95 °C and 5.25 °C to 88.95 °C, respectively. These findings provide important theoretical guidance for the design of precise temperature probes gauging fluorescent-phosphorescent ratios by regulating perturbed molecular conformations.

Introduction

Dual-emission materials with fluorescence and phosphorescence properties combine the rapid response of fluorescence with the long-lived afterglow characteristic of phosphorescence.[1] These materials have attracted much attention recently due to their potential applications in anti-counterfeiting,[2] display technologies,[3] sensing,[4–12] and bioimaging.[13] However, it is still challenging to create dual-emissive materials with a high phosphorescence quantum yield (Φ_p) and an ultralong phosphorescence lifetime (τ_p) under ambient conditions because the singlet–triplet transition in pure organic molecules is spin-forbidden, and triplet excitons tend to undergo non-radiative decay under ambient conditions.[14–16] The Φ_p and τ_p values of organic/polymeric luminescent materials can be improved by enhancing spin–orbit coupling (SOC), promoting intersystem crossing (ISC), and stabilizing triplet excitons. Therefore, the introduction of heavy atoms or heteroatoms with lone-pair electrons and the creation of unique molecular aggregates are crucial strategies for achieving high-performance fluorescent-phosphorescent dual-emissive materials.[17–24] However, enhancing SOC to promote ISC, which improves phosphorescence efficiency, often results in a shorter phosphorescence lifetime.[25] Therefore, precise design guidelines for producing high-performance fluorescent-phosphorescent dual-mode emissive materials are highly desirable.

To investigate the connection between molecular structures and phosphorescent qualities, Yang's group[26] synthesized thianthrene and its oxygen-substituted analogues, phenoxathiin and dioxin. The folding angles of these three luminogens were determined to be 126.05°, 143.44° and 180°, respectively, by systematic investigation. These compounds exhibited room-temperature phosphorescence

[a] School of Chemistry, South China Normal University, Guangzhou, 510006, P. R. China. E-mail: zhoujd@scnu.edu.cn, shg73@163.com
[b] School of Environmental and Chemical Engineering, Wuyi University, Jiangmen 529020, P. R. China. E-mail: bingjiaxu@m.scnu.edu.cn
[c] Institute of Biological and Medical Engineering, Guangdong Academy of Sciences, Guangzhou 510316, China
† These authors contributed equally to this work.

(RTP) quantum yields of 31.3%, 1.2%, and 0%, respectively, when doped in amorphous polymethyl methacrylate films. These results demonstrated that the folded conformation can enhance the RTP efficiency, but the lifetime is only at the millisecond level. Through precise control of molecular packing density and SOC, Su's group[27] synthesized phenoxathiin and its borate ester derivatives, obtaining a high RTP quantum yield of 20% in single crystals, but with a limited lifetime of 20 ms. It can be seen that the folded phenoxathiin and thianthrene derivatives can enable purely organic RTP emission by simultaneously enhancing ISC and stabilizing triplet excitons through their fold-enhanced SOC mechanism. Nevertheless, the performance of such SOC-enhanced RTP materials is still constrained by the lack of universal molecular design principles. Therefore, developing rational molecular design strategies to achieve high Φ_p and ultralong τ_p remains an urgent priority concurrently. On the other hand, systematic investigations reveal that polycyclic aromatic hydrocarbons (PAHs), such as phenanthrene (Phen) and triphenylene (TP), have planar and rigid structures that efficiently inhibit molecular vibrations, leading to highly efficient luminophores.[28–30] Hence, to achieve a dual-mode fluorescence-phosphorescence emission, it is an involuntary strategy to link the fluorescent PAH and the folded POX units that offer the ISC channels.

In this work, two organic luminogens, POXPhen and POXTP, were designed, synthesized, and then doped into a melamine-formaldehyde (MF) polymer to create dual-emission materials. The MF polymer can isolate moisture and oxygen to stabilize triplet excitons, provide an external rigid environment to restrict intramolecular motions, and optimize the folded conformation of the POX segment by utilizing the various steric hindrances and van der Waals forces generated by the polycyclic segments. The resulting polymer materials, POXPhen@MF and POXTP@MF, exhibit a high Φ_p of 20.32% and 25.08%, as well as ultralong τ_p of 1.60 s and 1.20 s, respectively. In comparison, the lifetimes were 35.07 ms and 31.58 ms, respectively, when POX: Phen/TP was blended at a mass ratio of 1 : 1 (non-covalent bonding). The relationship between molecular conformation and emission properties was also investigated. The temperature-dependent conformational perturbations and distributions varied from the folded angle of the POX unit and the rotational angles between the POX and PAH units, leading to a linear temperature-response towards fluorescence and phosphorescence intensities, which expands the application scenarios of dual-emission materials with fluorescence and phosphorescence in sensing.

Results and discussion

The POX unit was functionalized by adding either a Phen or a TP moiety, and the target POXPAH compounds, POXPhen and POXTP (Fig. 1a), were synthesized *via* a Suzuki–Miyaura cross-coupling reaction (Scheme S1). The final products were purified by silica gel column chromatography and recrystallization. Their chemical structures and sample purity were fully characterized through ^{1}H nuclear magnetic resonance spectroscopy, high-resolution mass spectrometry and high-performance liquid chromatography (HPLC).

The steady-state PL spectra of POXPhen and POXTP crystals exhibit the emission peak at 417 nm and 395 nm, respectively, under 300 nm UV excitation (Fig. S1). In addition, the lifetime decay curves revealed that the longest lifetimes corresponding to these emission peaks are on the nanosecond scale, confirming that the emission peaks of POXPhen and POXTP crystals originate from fluorescent processes (Fig. S2).

The UV-visible absorption spectra of the luminogens in different dilute solutions (10^{-5} M) are provided in Fig. S3. POXPhen displays an intense absorption band at 297 nm, which can be attributed to π–π^* transitions of the molecules. Meanwhile, an absorption tail is also observed in the region above 300 nm, which likely originates from charge transfer (CT) transitions (*vide infra* in the theoretical discussion). POXTP displays structureless absorption bands, but a similar shape with a small red shift related to POXPhen. Notably, the properties of the localized excited (LE) and charge transfer (CT) transitions in dilute solutions are confirmed by the fact that both compounds exhibit almost identical absorption profiles over a range of different solvent polarities. The fluorescent and phosphorescent properties of POXPhen and POXTP were investigated through steady-state PL and delayed emission spectra at 77 K in tetrahydrofuran (THF) solutions (Fig. S4). The steady-state PL spectra displayed dual-emission peaks at 372/544 nm for POXPhen and 385/497 nm for POXTP, while the corresponding delayed spectra only showed single emissive peaks at 544 nm and 497 nm, respectively, which are attributed to the phosphorescent bands. Meanwhile, the steady-state PL spectra and delayed emission spectra of POXPhen and POXTP presented substantial overlap in frozen THF solutions, indicating that POXPhen and POXTP have strong SOC and potential to achieve efficient RTP. To verify this hypothesis, POXPhen and POXTP were employed as guest molecules and doped into the MF polymer matrix, respectively. The rigid three-dimensional covalent network of the MF polymer is capable of restricting molecular motions to suppress non-radiative decays, thereby enabling efficient RTP of POXPhen and POXTP under ambient conditions. The doping concentrations of the guest luminogens were subsequently optimized. The emission of pure MF film is extremely weak and negligible (Fig. S5a–d). The optimal doping concentrations for POXPhen@MF and POXTP@MF are 0.05% and 0.10%, respectively, as the intensities of their steady-state and delayed PL spectra reach the maximum, with long lifetimes of 1.60 s and 1.20 s (Fig. S5b, d, and f). In addition, the wavelengths of the POXPhen@MF and POXTP@MF delayed emission peaks remain essentially unchanged as the doping concentration increases (Fig. S5). These observations indicate that the phosphorescence of POXPhen@MF and POXTP@MF probably originates from single molecules of the guest luminogens. The POXPhen@MF and POXTP@MF films with optimal doping concentrations were subjected to the following study.

The steady-state PL spectra and delayed emission spectra of POXPhen@MF and POXTP@MF exhibit significant overlap, as illustrated in Fig. 1b and c. Their calculated ISC rate constants

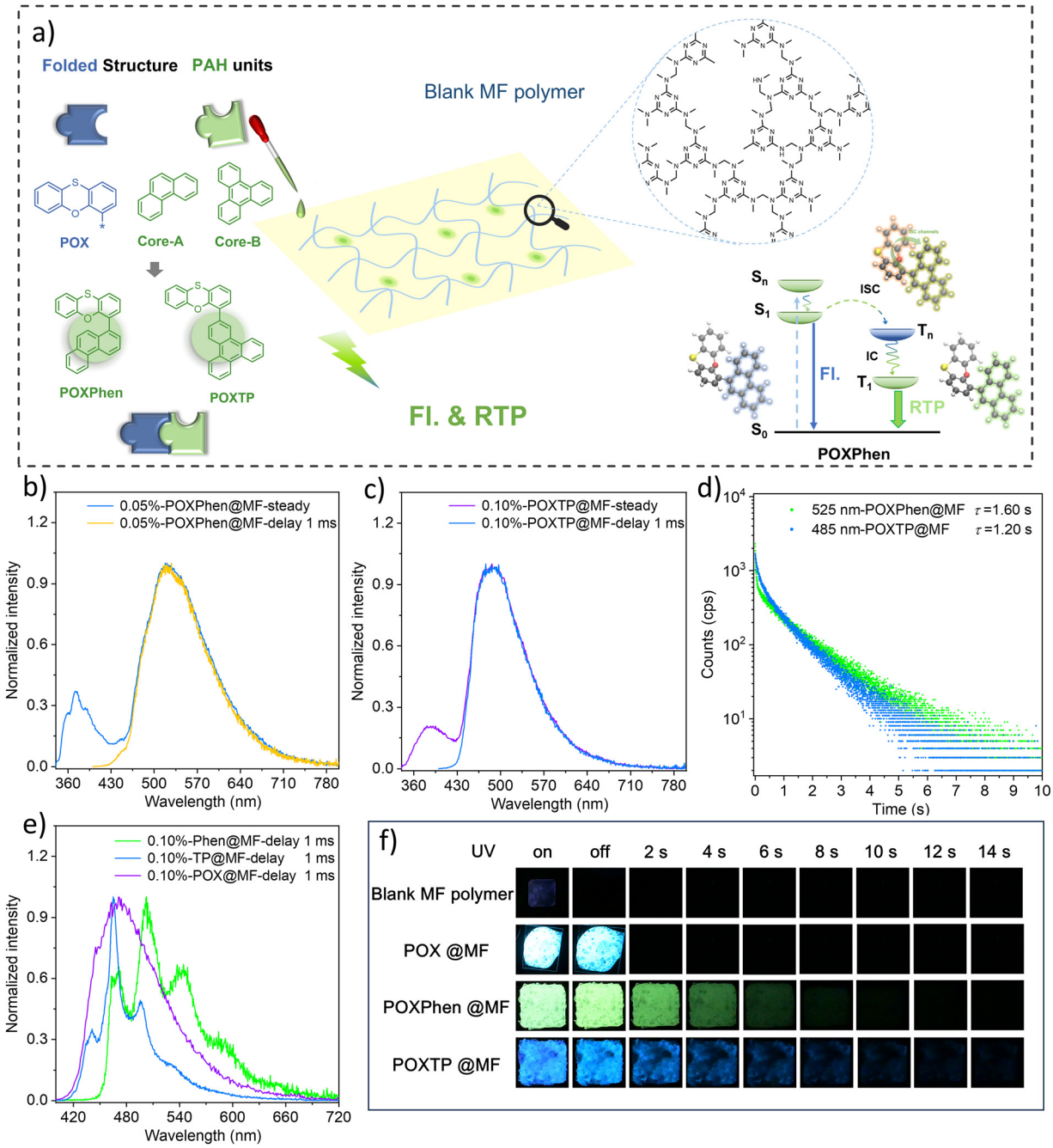

Fig. 1 (a) Chemical structures of POXPAH compounds and the schematic of small molecules doped in the MF polymer with a 3D covalent network, and the mechanism diagram of POXPhen@MF. (b) and (c) Steady-state PL spectra and the delayed emission spectra (delayed 1 ms) of POXPhen@MF and the POXTP@MF with the optimal doping concentration. (d) Delayed emission decay curves and lifetimes of POXPAH@MF with the optimal doping concentration (excitation: 300 nm). (e) Delayed emission spectra (delayed 1 ms) of 0.10%-POX@MF, 0.10%-Phen@MF and 0.10%-TP@MF (excitation: 300 nm). (f) Afterglow images of the blank MF polymer, POX@MF, POXPhen@MF and POXTP@MF (excitation: 310 nm).

are 15.7×10^6 s^{-1} and 16.3×10^6 s^{-1}, suggesting efficient ISC processes. The Φ_p values of POXPhen@MF and POXTP@MF under ambient conditions are 20.32% and 25.08%, respectively, while the Φ_{fluo} values under ambient conditions are 4.34% and 3.77% (Table S1). The delayed emission peak of POXPhen@MF at 525 nm has a lifetime of 1.60 s, and the delayed emission peak of POXTP@MF at 485 nm has a lifetime of 1.20 s (Fig. 1d). Afterglow luminescence images of POXPAH@MF and POX@MF under identical conditions are shown in Fig. 1f. Notably, the host–guest doping strategy enables ultralong and efficient RTP of POXPhen and POXTP when utilizing the rigid MF polymer as the host. The steady-state emission peak of POXPhen@MF at 372 nm has the longest lifetime of 12.95 ns, while that of POXTP@MF at 385 nm has the longest lifetime of 15.38 ns, both of which are at the nanosecond level, as illustrated in Fig. 1b, c and Fig. S6. These results indicate that the

steady-state emission peaks of POXPAH@MF in the near-ultraviolet region stem from fluorescence. Therefore, by introducing fused-ring segments with different sizes into the POX moiety and embedding the resulting luminophores into the MF polymers, it may be possible to regulate the SOC of the molecules and thereby enable efficient ultralong RTP, resulting in fluorescence-phosphorescence dual emissions. The effects of excitation wavelength and time on delayed emission were investigated, as shown in Fig. S7 and S8. The wavelengths of the delayed emission peaks in the excitation-delayed emission maps of POXPhen@MF and POXTP@MF remain invariant to the excitation wavelengths. These results further confirm that the phosphorescence center is the guest molecule in a monomolecular state. Notably, POXPhen@MF and POXTP@MF have similar excitation wavelengths, which may be due to the important role of the POX segment in the excitation process. Photophysical properties of POX@MF were then investigated to further validate the luminescent centers of POXPhen and POXTP. The steady-state PL spectra of POX@MF completely overlap with its delayed emission spectra, exhibiting efficient and pure organic RTP with an emission peak at 471 nm, as shown in Fig. S9. However, the lifetime of this blue phosphorescent peak is only 38.41 ms. Moreover, ultralong RTP could be not observed when POX was physically blended with Phen or TP at a 1 : 1 ratio and subsequently doped into the MF polymer films. The phosphorescence lifetimes of the resulting materials were only 35.07 ms and 31.58 ms, respectively (Fig. S10), which indicated the inefficient energy transfer from POX to PAH for ultralong RTP. In sharp contrast, when POX is covalently linked to Phen/TP and the resulting guest molecules POXPhen and POXTP are doped into MF polymer matrices, efficient RTP with high Φ_p and ultralong τ_p is achieved. This is because n–π* transitions are promoted by the introduction of POX, which has a fold-induced enhanced SOC impact. In essence, heterocyclic compounds with folded geometry enable ISC processes involving geometrical planarization from the singlet to the triplet excited states, which are dependent on the folded angle. This facilitates the enhancement of SOC and thus the ISC process to increase the population of triplet excitons.[26,30–32] Meanwhile, intramolecular charge transfer occurs between the planar rigid Phen/TP fragments and the POX fragment, generating CT intermediates. The steric hindrance imposed by Phen and TP units effectively inhibits intramolecular rotation and diminishes non-radiative decay pathways, thereby promoting the ISC processes. In addition, by comparing the delayed emission spectra of POX@MF and POXPAH@MF, it is found that the delayed emission spectrum of POXPhen@MF has a greater degree of overlap with that of Phen@MF, which preliminarily indicates that most of the phosphorescence emission centers are concentrated in the Phen segment, and a small part is concentrated in the POX segment. However, the delayed emission spectrum of POXTP@MF shows a similar degree of overlap with those of POX@MF and TP@MF, which preliminarily indicates that the TP acts as a phosphorescence emission center (Fig. 1b–e). POXPhen and POXTP were subsequently doped into an epoxy polymer (EP) matrix to explore the universality of guest molecules, and their steady-state and delayed emission spectra, as well as delayed emission decay curves, were recorded. The steady-state PL spectra and delayed emission spectra of POXPhen@EP and POXTP@EP are almost identical to those of POXPhen@MF and POXTP@MF, with delayed emission lifetimes of 1.51 s and 1.03 s (Fig. S11), respectively. It is evident that doping POXPhen and POXTP into the EP polymer can also result in ultralong and efficient RTP. These results indicate that the inherent properties of POXPhen and POXTP are responsible for the excellent afterglow performance of these polymer films under ambient conditions, while the polymer matrix mainly provides a rigid environment to inhibit molecular motions.

Molecular conformations of POXPhen and POXTP were optimized by scanning the torsion angle between the POX and aromatic hydrocarbons of Phen or TP to survey their influence on the photophysical processes (Fig. 2a and b).[33] The theoretical calculation results indicate that there are indeed four conformations for the phenoxazine derivatives. Such observations may be attributed to the conformation inversion of the POX segment and rotation of the Phen/TP moiety. Among them, two conformations are symmetrically equivalent to each other, exhibiting the same ground state (Fig. S12). Therefore, subsequent studies were performed using POXPhen-1, POXPhen-2, POXTP-1, and POXTP-2. The intermolecular forces within the molecule were analyzed through the interaction region indicator (IRI) function (Fig. S13).[34] There is a large steric hindrance between the POX segment and PAH units, indicating multiple molecular conformations of POXPAH. The ground state and excited state information of the molecule was analyzed using POXTP-1 and POXTP-2 as examples. As shown in Table S2, POXTP-2 shows higher electronic energy than POXTP-1, with a potential energy barrier difference (ΔE) of 24 meV. These results indicate that the conformational conversion from POXTP-1 to POXTP-2 is possible at 298.15 K (RT = 25.69 meV), leading to a conformational distribution of POXTP at room temperature. By contrast, the ΔE between POXPhen-1 and POXPhen-2 is calculated to be 84 meV, suggesting that the molecular conformational conversion from POXPhen-1 to POXPhen-2 is more difficult and may require external energy, for instance, UV light excitation. As shown in Fig. S12 and Table S2, with the increase in the number of benzene rings in POXPAH, the folding angle (β) of the two phenyl rings on the POX segment in POXTP is slightly larger than that in POXPhen, and the torsion angles (α) between the POX segment and PAH moieties are different. These calculated results may be associated with the different steric hindrance and van der Waals forces between the Phen/TP unit and the POX segment. Accordingly, the ISC efficiency of POXPAH is likely related to the folding angle of the POX segment.[26,33]

In order to investigate the photophysical properties of POXPAH, the configurations of POXPhen-1, POXPhen-2, POXTP-1, and POXTP-2 in the T_1 excited state were optimized, and the emission properties were quantified using the corresponding transition energies from the T_1 to S_0 states (Fig. 2c and d), which match the spectral results. The natural

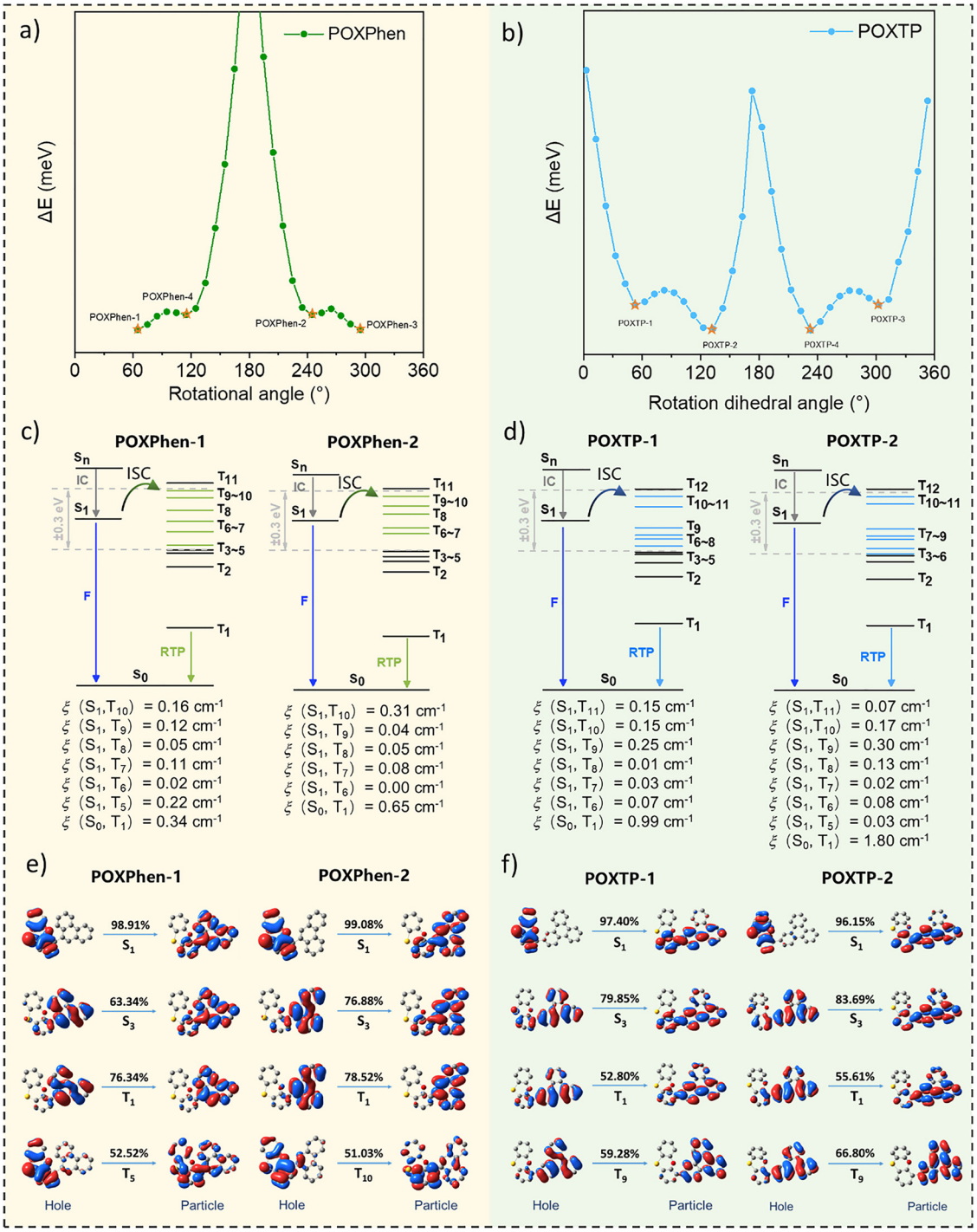

Fig. 2 (a) and (b) Potential surface scanning calculations for the compounds POXPhen and POXTP at the S_0 state, where the torsion angle between POX and Phen/TP served as the scanning coordinate. (c) and (d) Diagram of the calculated energy levels, possible ISC channels, and SOC constants between the singlet and triplet excited states of a single molecule for POXPhen-1, POXPhen-2, POXTP-1 and POXTP-2. (e) and (f) NTO characteristics for S_n and T_n states of the single molecule of POXPhen and POXTP and their corresponding transition probabilities.

transition orbits (NTOs) of S_n and T_n in POXPAH were analyzed. As shown in Fig. 2e and f, POXPAH-1 exhibits similar transition characteristics to POXPAH-2. Hereinafter, POXPAH-2 is considered as an example to analyze its excitation and emission properties. Under UV light excitation, POXPhen-2 preferentially transitions to the S_3 excited state based on the largest oscillator strength. Its NTOs show excitation properties of the ^{1}LE state consistent with the experimental results, and both electrons and holes in the S_3 excited states are distributed on the PAH fragment. In the NTOs of the T_1 excited state of POXPhen, most of the electrons and holes are concentrated on the Phen moiety, and a small part is on the POX fragment. In the NTOs of the T_1

energy level of POXTP, electrons and holes are partially concentrated on the TP unit and partially in the POX fragment. These observations indicate that the phosphorescence emission centers of POXPhen and POXTP are located mainly in the PAH fragments, which is consistent with the experimental results. These results confirm that the PAH fragment plays a dominant role in the excitation and emissive process, resulting in similar excitation-delayed emission maps for POXPhen@MF and POXTP@MF.

As the S_3 excited state rapidly relaxes to the S_1 excited state, the distribution of electrons and holes is transferred from PAH to POX moieties, indicating the intramolecular charge transfer process. Due to the fold-induced enhanced SOC effect, excitons in the S_1 excited state of the POX fragment rapidly undergo ISC to T_n and relax to the T_1 excited state through internal conversion (IC), generating more triplet excitons on the PAH fragment. In the electron transition process, CT characteristics were observed from POX to Phen/TP (Fig. 2c and d). Moreover, some potential ISC channels from S_1 to T_n are found, where the energy gaps are small enough for electron transition.[25] Interestingly, the NTO pairs of T_n also show the CT characteristics (Fig. 2e and f). In this context, excited-state features involving intramolecular charge transfer (ICT) between POX and PAHs probably facilitate the integration of the excitation characteristics of the two chromophores, leading to efficient dual-emissive materials with luminescent centers located on both POX and PAH fragments. Compared with the radiative energy transfer process in the non-covalently linked POX and PAH system, the linked POXPAH with photoexcited ICT properties is more conducive to achieving dual-mode emission on the POX and PAH fragments. Therefore, when introducing planar and rigid PAHs on the POX unit, a chromophore with folding-induced SOC enhancement properties, the excitons at the S_1 excited state can quickly reach the T_1 excited state *via* ISC, thereby generating abundant triplet excitons at the PAH units. The excited states of the luminogens exhibit mainly the characteristics of PAH, resulting in high-performance fluore scence-phosphorescence dual-mode emission under ambient conditions. These results thus provide helpful guidance for achieving efficient multimode emissions at room temperature by regulating the conformations of organic luminogens with folding-induced SOC-enhancement properties, like phenoxathiin and thianthrene derivatives.

Ratiometric probes based on fluorescence-phosphorescence dual-mode emission are promising for temperature sensing due to their self-referencing capability. High Φ_p, spectrally distinct emission peaks with minimal mutual interference, and a well-defined linear response are necessary for the optimal ratiometric fluorescence-phosphorescence temperature probe.[35–40] However, their performance is constrained by intrinsic material properties, the trade-off between lifetime and efficiency, as well as complexities in fabrication and application. Fan's group[36] integrated two fluorescent dyes with distinct temperature-dependent responses to fabricate a flexible thin-film ratiometric fluorescence temperature sensor with a wide operational range of 20–240 °C. However, the fluorescence intensity ratio was the only sensing modality in this system. Makoto Tadokoro's group[37] synthesized a series of novel tetranuclear zinc(II) cluster probes that exhibited unique dual-emissive characteristics of fluorescence-phosphorescence in the low-temperature range (77–200 K). These probes exhibited high phosphorescence efficiency and self-calibration, but were limited by low-temperature applicability.

Due to the interference between phosphorescence and fluorescence, intersystem and radiative processes can be

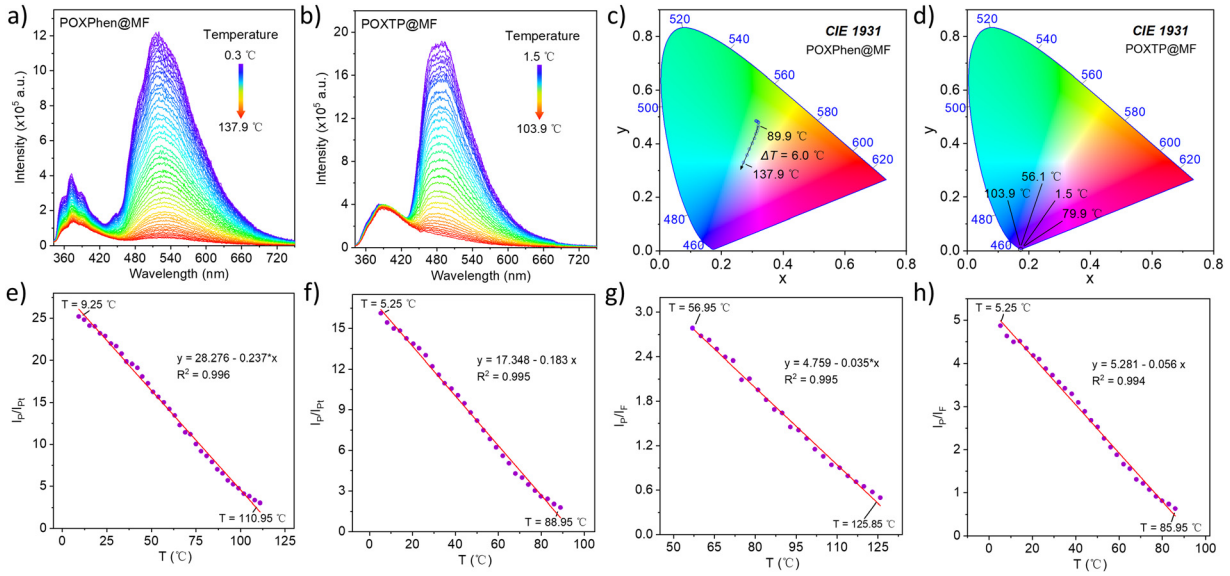

Fig. 3 (a) and (b) Steady-state PL spectra of POXPhen@MF and POXTP@MF at different temperatures (excitation: 300 nm). (c) and (d) $CIE_{x,y}$ chromaticity coordinates of POXPhen@MF and POXTP@MF at different temperatures. (e) and (f) Plots of I_P/I_{Pt} *versus* T for POXPhen@MF and POXTP@MF (I_{Pt} of POXPhen@MF is the phosphorescence intensity at 525 nm at 137.9 °C, I_{Pt} of POXTP@MF is the phosphorescence intensity at 485 nm at 103.9 °C). (g) and (h) Plots of I_P/I_F *versus* T for POXPhen@MF and POXTP@MF.

affected by tuning the conformational perturbation and distribution related to the environmental temperature.[41] The steady-state PL spectra of POXPhen@MF and POXTP@MF films were recorded at various temperatures. The phosphorescence emission of POXPhen@MF and POXTP@MF disappeared at 137.90 °C and 103.90 °C, respectively, but the fluorescence emission was almost unchanged, demonstrating the high temperature resistance properties of the dual-mode emission (Fig. 3a and b). According to the $CIE_{x,y}$ chromaticity diagrams obtained from spectral conversion, the variations in the emission color of POXPhen@MF and POXTP@MF are not noticeable with varying temperature. By contrast, the ratios of the phosphorescence intensity to final phosphorescence intensity (I_P/I_{Pt}) for POXPhen@MF and POXTP@MF decrease linearly with the elevation in temperature in the ranges of 9.25–110.95 °C and 5.25–88.95 °C, respectively. These observations suggest that the doped polymer films can be used as temperature probes based on the change in phosphorescence intensity. Furthermore, it is found that the related intensities of phosphorescence to fluorescence (I_P/I_F) for POXPhen@MF and POXTP@MF also decrease linearly with the elevation in temperature in the ranges of 56.95–125.85 °C and 5.25–85.95 °C, respectively, indicating that the doped polymer films can also serve as temperature probes by utilizing the dual-mode emission properties. Accordingly, POXPhen@MF and POXTP@MF enable wide-range temperature sensing through their unique photophysical properties, including fluorescence-phosphorescence dual-mode emission, high Φ_p values, and high-temperature phosphorescence, which significantly expand the application scenario of phosphorescence materials in the field of sensing.

Conclusions

In summary, POXPAH luminogens, composed of fluorescent PAH and POX moieties, were designed and synthesized, of which the planar PAH groups present the intense emissive properties, and the folded POX unit shows the folding-induced SOC enhancement properties. The ISC efficiencies of the resulting luminogens are related to their molecular conformations, especially the folded angle of POX and the rational angle between the POX and PAH fragments, which show temperature-reliable conformational perturbation and distribution. As a result, the doped polymer films exhibit efficient dual-mode fluorescence-phosphorescence emission and present a linear response to temperature. This work may provide helpful guidance for the development of luminescent polymer materials with efficient RTP and multi-mode emissions using organic chromophores with folding-induced enhanced SOC properties, such as POX and thioanthracene, and rigid, planar PAHs to construct guest luminogens.

Author contributions

Yuling Huang: writing – original draft, conceptualization, methodology and data curation. Huiwen Zeng: formal analysis and data curation. Yu Lang: formal analysis. Cong Liu: writing – review & editing. Zixuan Ran: data curation. Fayong Li: formal analysis. Jiadong Zhou: writing – review & editing. Bingjia Xu: writing – review & editing, funding acquisition, supervision and methodology. Guang Shi: funding acquisition and conceptualization.

Conflicts of interest

There are no conflicts to declare.

Data availability

The data supporting this article, comprising the synthesis, chemical structure characterization, and photophysical properties of the compounds, have been included as part of the supplementary information (SI). Supplementary information is available. See DOI: **https://doi.org/10.1039/d5qm00618j**.

Data are available from the authors upon request.

Acknowledgements

This work was supported by the National Natural Science Foundation of China (52473194) and the Guangdong Basic and Applied Basic Research Foundation (2023A1515010915 and 2024A1515010047).

Notes and references

1 P. Jiang, Y. Liu, B. Ding and X. Ma, Regulation strategies of dynamic organic room-temperature phosphorescence materials, *Chem. Biochem, Eng. Q.*, 2024, **1**, 13–25.
2 X. Hua, J. Yi and Y. Ni, Construction of delayed fluorescence/phosphorescence dual-mode carbon dots and its application in paper anti-counterfeiting systems, *Appl. Mater. Today.*, 2024, **39**, 102309.
3 Y. Yu, Z. Li, W. Zhou, S. Wei and T. Chen, Electricity/light-heat-hygro multi-responsive soft luminescent systems for rewritable and programmable information display, *Chem. Eng. J.*, 2024, **490**, 151742.
4 C. Li, X. Li and Q. Wang, Supramolecular self-assembling strategy for constructing cucurbit[6]uril derivative-based amorphous pure organic room-temperature phosphorescence complex featuring extra-high efficiency, *Chin. Chem. Lett.*, 2022, **33**, 877–880.
5 W. Qin, J. Ma, Y.-S. Zhou, Q. Hu, Y. Zhou and G. Liang, Simultaneous promotion of efficiency and lifetime of organic phosphorescence for self-referenced temperature sensing, *Chem. Eng. J.*, 2020, **400**, 125934.
6 C. Si, T. Wang, A.-K. Gupta, D.-B. Cordes, A.-M.-Z. Slawin, J.-S. Siegel and E. Zysman-Colman, Room-Temperature Multiple Phosphorescence from Functionalized Corannulenes: Temperature Sensing and Afterglow Organic Light-Emitting Diode, *Angew. Chem., Int. Ed.*, 2023, **62**, e202309718.
7 W. Miao, B. Liu, H. Li, S. Zheng, H. Jiao and L. Xu, Fluorescent Eu^{3+}/Tb^{3+} Metal-Organic Frameworks for

Ratiometric Temperature Sensing Regulated by Ligand Energy, *Inorg. Chem.*, 2022, **61**, 14322–14332.
8 Y. Yang, L. Chen, F. L. Jiang, M. Yu, X. Wan, B. Zhang and M. Hong, A family of doped lanthanide metal–organic frameworks for wide-range temperature sensing and tunable white light emission, *J. Mater. Chem. C*, 2017, **5**, 1981–1989.
9 J. Ma, Y. Zhou, H. Gao, F. Zhu and G. Liang, Full-type photoluminescence from a single organic molecule for multi-signal temperature sensing, *Mater. Chem. Front.*, 2021, **5**, 2261–2270.
10 B.-P. Debata, M.-D. Thiyagarajan, R. Prathap, J.-D. Girase, S.-K. Iyer, S. Patel and S. Vaidyanathan, Benzil-imidazole blue fluorophores and their applications in blue/white light-emitting diodes, sensing and anticounterfeiting, *J. Mater. Chem. C*, 2025, **13**, 2711–2731.
11 Y. Gao, W. Ye, K. Qiu, X. Zheng, S. Yan, Z. Wang, Z. An, H. Shi and W. Huang, Regulating isolated-molecular and aggregated-state phosphorescence for multicolor afterglow by photoactivation, *Adv. Mater.*, 2023, **35**, 2306501.
12 F. Nie, B. Zhou and D. Yan, Ultralong room temperature phosphorescence and reversible mechanochromic luminescence in ionic crystals with structural isomerism, *Chem. Eng. J.*, 2023, **453**, 139806.
13 Z. Guan, Z. Tang, J. Deng, Y. Zheng, H. Li and X. Liu, Multicolor pure organic room temperature phosphorescent materials with long lifetime and high efficiency, *Adv. Funct. Mater.*, 2024, **34**, 2310198.
14 Y. Gao, Q. Zhang, F. Wang and P. Sun, Wide-range tunable phosphorescence emission in cellulose-based materials enabled by complementary-color phosphors, *Chem. Eng. J.*, 2023, **471**, 144665.
15 X. Yang, S. Wang, K. Sun, H. Liu, M. Ma, S. Zhang and B. Yang, A Heavy-atom-free Molecular Motif Based on Symmetric Bird-like Structured Tetraphenylenes with Room-Temperature Phosphorescence (RTP) Afterglow over 8 s, *Angew. Chem., Int. Ed.*, 2023, **135**, e202306475.
16 J. Yu, Z. Sun, H. Ma, C. Wang, W. Huang, Z. He, W. Wu, H. Hu, W. Zhao and W. Zhu, Efficient visible-light-activated ultra-long room-temperature phosphorescence triggered by multi-esterification, *Angew. Chem., Int. Ed.*, 2023, **62**, e202316647.
17 D. Ma, Z. Li, K. Tang, Z. Gong, J. Shao and Y. Zhong, Nylons with highly-bright and ultralong organic room-temperature phosphorescence, *Nat. Commun.*, 2024, **15**, 4402.
18 Y. He, J. Wang, Q. Li, S. Qu, C. Zhou, C. Yin, H. Ma, H. Shi, Z. Meng and Z. An, Highly efficient room-temperature phosphorescence promoted via intramolecular-space heavy-atom effect, *Adv. Opt. Mater.*, 2023, **11**, 2201641.
19 H. Zhang, S. Wu, Y. Liang, Z. Zhang, H. Wei, Q. Yang, P. Hu, C. Liu, Z. Yang, C. Zheng, G. Shi, Z. Chi and B. Xu, Enabling efficient and ultralong room-temperature phosphorescence from organic luminogens by locking the molecular conformation in polymer matrix, *Chem. Eng. J.*, 2024, **497**, 154949.
20 Z. He, H. Gao, S. Zhang, S. Zheng, Y. Wang, Z. Zhao, D. Ding, B. Yang, Y. Zhang and W. Yuan, Achieving persistent, efficient, and robust room-temperature phosphorescence from pure organics for versatile applications, *Adv. Mater.*, 2019, **31**, 1807222.
21 A. Abe, K. Goushi, M. Mamada and C. Adachi, Organic binary and ternary cocrystal engineering based on halogen bonding aimed at room-temperature phosphorescence, *Adv. Mater.*, 2024, **36**, e2211160.
22 J. Chen, Y. Zhang, S. Zhang, G. Liu, Q. Sun, S. Xue and W. Yang, Two-Phase Rubber-Plastic MaTPces' Stabilization of Organic Room-Temperature Phosphorescence Afterglows Better than Plastic Matrix, *Small Struct.*, 2023, **4**, 2300101.
23 S. Zhang, W. Yao, A. Lv, K. Liu, Y. Zhang, C. Zhou, H. Ma, H. Shi and Z. An, Achieving highly efficient long-wavelength phosphorescence emission of large singlet-triplet energy gap materials by host-guest doping, *Sci. China: Chem.*, 2024, **67**, 1922–1928.
24 R. Blau, O. Shelef and D. Shabat, Chemiluminescent probes in cancer biology, Chemiluminescent probes in cancer biology, *Nat. Rev. Bioeng.*, 2023, **1**, 648–664.
25 H. Zeng, H. Li, P. Zhen, J. Zhou, B. Xu, G. Shi, Y. Zhang, Z. Chi and C. Liu, Tuning intramolecular charge transfer and suppressing rotations in thianthrene derivatives for enhancement of room-temperature phosphorescence, *Chem. Sci.*, 2025, **16**, 9169–9177.
26 G. Pan, Z. Yang, H. Liu, Y. Wen, X. Zhang, Y. Shen, C. Zhou, S. Zhang and B. Yang, Folding-induced spin–orbit coupling enhancement for efficient pure organic room-temperature phosphorescence, *J. Phys. Chem. Lett.*, 2022, **13**, 1563–1570.
27 M. Li, X. Cai, Z. Qiao, K. Liu, L. Wang, N. Zheng and S. Su, Achieving high-efficiency purely organic room-temperature phosphorescence materials by boronic ester substitution of phenoxathiine, *Chem. Commun.*, 2019, **55**, 7215–7218.
28 H. Huang, N. Li, S. Fu, X. Mo, X. Cao, X. Yin and C. Yang, Pure Polycyclic Aromatic Hydrocarbon Isomerides with Delayed Fluorescence and Anti-Kasha Emission: High-Efficiency Non-Doped Fluorescence OLEDs, *Adv. Sci.*, 2023, **10**, 2304204.
29 Y. Hu, M. Huang, H. Liu, J. Miao and C. Yang, Narrowband fluorescent emitters based on BN-doped polycyclic aromatic hydrocarbons for efficient and stable organic light-emitting diodes, *Angew. Chem., Int. Ed.*, 2023, **135**, e202312666.
30 Y. Wu, J. Liu, G. Yang, Z. Bin and J. You, Aromaticity Localization Effects in Polycyclic Aromatic Hydrocarbons for Discovering Narrowband Fluorescence Materials, *J. Am. Chem. Soc.*, 2025, **147**, 19305–19314.
31 H. Liu, Y. Gao, J. Cao, T. Li, Y. Wen, Y. Ge, L. Zhang, G. Pan, T. Zhou and B. Yang, Efficient room-temperature phosphorescence based on a pure organic sulfur-containing heterocycle: Folding-induced spin–orbit coupling enhancement, *Mater. Chem. Front.*, 2018, **2**, 1853–1858.
32 S. Zhao, Z. Yang, X. Zhang, H. Liu, Y. Lv, S. Wang, Z. Yang, S. Zhang and B. Yang, A functional unit combination strategy for enhancing red room-temperature phosphorescence, *Chem. Sci.*, 2023, **14**, 9733–9743.
33 T. Lu, Molclus program, Version 1.12, **https://www.keinsci.com/research/molclus.html** (accessed July 15, 2025).

34 T. Lu and Q. Chen, Interaction Region Indicator: A Simple Real Space Function Clearly Revealing Both Chemical Bonds and Weak Interactions, *Chem. Methods*, 2021, **1**, 231–239.
35 H. Liu, G. Pan, Z. Yang, Y. Wen, X. Zhang, S. Zhang, W. Li and B. Yang, Dual-Emission of Fluorescence and Room-Temperature Phosphorescence for Ratiometric and Colorimetric Oxygen Sensing and Detection Based on Dispersion of Pure Organic Thianthrene Dimer in Polymer Host, *Adv. Opt. Mater.*, 2022, **10**, 2102814.
36 X. Qian, M. Kong, L. Song, G. Yue, Y. Zhang, Y. Qian and Q. Fan, Heat Resistant Organic Dyes for High Temperature Luminescent Temperature Sensing, *Adv. Sens. Res.*, 2024, **3**, 2300143.
37 F. Kobayashi, Y. Takatsu, D. Saito, M. Yoshida, M. Kato and M. Tadokoro, Dual Emission with Efficient Phosphorescence Promoted by Intermolecular Halogen Interactions in Luminescent Tetranuclear Zinc (II) Clusters, *Inorg. Chem.*, 2024, **63**, 15323–15330.
38 K. Zhong, L. Yang, X. Hu, Y. Li, L. Tang, X. Sun, X. Li, J. Zhang, Y. Meng, R. Ma, S. Wang and J. Li, A colorimetric and NIR fluorescent probe for ultrafast detecting bisulfite and organic amines and its applications in food, imaging, and monitoring fish freshness, *Food Chem.*, 2024, **438**, 137987.
39 H. Li, M. Li, S. Zhang, M. Chen and J. Wang, Packaged europium/fluorescein-based hydrogen bond organic framework as ratiometric fluorescent probe for visual real-time monitoring of seafood freshness, *Talanta*, 2024, **272**, 125809.
40 M. Ji and X. Ma, Recent progress with the application of organic room-temperature phosphorescent materials, *Ind. Chem. Mater.*, 2023, **1**, 582–594.
41 J. Liang, J. Yang, Y. Wang, M. Shan, Z. Liu, J. Ren, M. Fang and Z. Li, Efficient photo-induced RTP materials based on phenothiazine and polycyclic aromatic hydrocarbons: Tunable emission color and thermal stimulus response, *Sci. China Mater.*, 2024, **67**, 2778–2788.

